

# Power Saving Techniques in 5G Technology for Multiple-Beam Communications

Olimpjon Shurdi, Alban Rakipi, and Algenti Lala

**Abstract**—The evolution of mobile technology and computation systems enables User Equipment (UE) to manage tremendous amounts of data transmission. As a result of current 5G technology, several types of wireless traffic in millimeter wave bands can be transmitted at high data rates with ultra-reliable and small latency communications. The 5G networks rely on directional beamforming and mmWave uses to overcome propagation and losses during penetration. To align the best beam pairs and achieve high data rates, beam-search operations are used in 5G. This combined with multibeam reception and high-order modulation techniques deteriorates the battery power of the UE. In the previous 4G radio mobile system, Discontinuous Reception (DRX) techniques were successfully used to save energy. To reduce the energy consumption and latency of multiple-beam 5G radio communications, we will propose in this paper the DRX Beam Measurement technique (DRX-BM). Based on the power-saving factor analysis and the delayed response, we will model DRX-BM into a semi-Markov process to reduce the tracking time. Simulations in MATLAB are used to assess the effectiveness of the proposed model and avoid unnecessary time spent on beam search. Furthermore, the simulation indicates that our proposed technique makes an improvement and saves 14% on energy with a minimum delay.

**Index terms**—User Equipment (UE), Discontinuous Reception (DRX), beamforming, multiple-beam communication.

## I. INTRODUCTION

**N**OWADAYS, energy, and information are two essential aspects of modern life, and their interaction has significant implications in society. While the volume of information transmitted through mobile networks continues to increase rapidly, the energy needed to support such growth has become a concern. According to Ericsson Mobility Report, mobile data traffic is expected to increase eightfold by 2023. Approximately 5 billion 5G subscriptions are expected globally, accounting for 55 percent of all mobile subscriptions by the end of 2028. In order to meet the high demand for mobile data traffic, the 3rd Generation Partnership Project (3GPP) has already standardized the use of a high-frequency band in 5G technology generation.

Manuscript received May 1, 2023; revised May 22, 2023. Date of publication June 30, 2023. Date of current version June 30, 2023.

Authors are with the Department of Electronics and Telecommunications, Polytechnic University of Tirana, Albania (e-mails: oshurdi@fti.edu.al, arakipi@fti.edu.al, alala@fti.edu.al).

Digital Object Identifier (DOI): 10.24138/jcomss-2023-0056

5G millimeter wave (mmWave) is not a very trodden spectrum but it promises large bandwidths and is an incredibly attractive field for 5G communications and beyond. However, 5G mmWave also poses propagation challenges. To address the UE capacity requirements, the 5G New Radio (NR) standard incorporates support for massive multiple-input multiple-output (mMIMO) technology and employs beam management techniques. These approaches aim to optimize throughput and enhance device density in the mobile network. The focus of [2] has mainly been on high spectrum bands, such as millimeter-wave frequencies; however, bands below 6 GHz will be crucial for delivering the required coverage and capacity.

It is widely accepted in both business and academia that, for 5G to succeed, a variety of spectrum assets spanning across low, medium, and high spectrum bands is necessary. Array antennas are needed at both the transmitter (Tx) and receiver (Rx) to implement beamforming for increasing the directivity of antenna, boosting signal power, and battling the poor propagation characteristics of higher-frequency signals. This allows the RF beam to propagate farther in that direction. As a result of this technique, non-line-of-sight (NLOS) RF communication in the mmWave spectrum can rely on reflection and/or diffraction of the beams to reach the UE. In case the direction becomes blocked, either due to the UE movement or changes in the environment, the beam may not be able to reach the UE. After the misalignment event, the beam search must begin to establish a connection. The main drawback of this method is that it requires use of computing resources, and it creates a bulky number of overheads that require implementation and management. Consequently, this leads to a higher energy consumption both during transmission and reception [3]. By using omnidirectional antennas there will be fewer overheads but with a lower frequency reuse factor.

It has been observed that during the long-term evolution (LTE) and 5G data traffic analysis, there is high bursty traffic which often results in a prolonged period of silence following an occasional transmission [4].

Over the past decade, several standardization and device implementation organizations have evaluated a series of energy-saving mobile device features. Especially, the 3GPP has implemented DRX as a significant energy-saving strategy for LTE mobile networks [5]. 5G technology uses the same protocol as previous LTE technology, that is, the UEs must, after synchronizations, decode the radio frame channel Physical

Downlink Control Channel (PDCCH) in order to verify that any data has been received. This method of wake-up decoding and data receiving will result in a larger energy consumption on the part of both the user and the base station (BS) [6].

The DRX mechanism allows the user to receive the data in DRX cycles. During the DRX cycle, the UEs monitor the PDCCH channel in one subframe after it turns into sleeping mode with most of the receiver circuits switched off in the remaining subframes [7].

In 5G, as in LTE, a receiver device has two main core network states as shown in Fig. 1 a): the Active state and the DRX state. When in active state, the receiver monitors periodically for paging messages and decodes the data into the frame. In DRX mode, the receiver may switch in several cycles. As shown in Fig. 1 b), in the DRX mode, each DRX sub-frame (cycle) is further subdivided into several states. As with the Active state, the Active time consists of two short periods: the "On-Duration state," in which the Rx reads the data after decoding the PDCCH he "Inactive time," in which the Rx remains awake while anticipating data. Once the inactivity time expires, the DRX technology steers the Rx to enter into one of the sleeping states. In 5G version 16 and beyond, there exist three types of sleeping states from which they can be chosen and modified by time interval from DRX: the first is Micro Sleep State directly after a PDCCH reception, the second is the Light Sleep State, and the Deep Sleep State. As in the LTE frame in the DRX, the sleeping times of each DRX cycle can be modified and derived by the network for diverse types of user profiles, providing different quality services.

This paper's contributions are summarized as follows. We present an innovative discontinuous reception strategy for high-frequency band multiple-beam communication systems. Our proposal is the steering of the Rx to conduct measurement via Radio Link Monitoring (RLM) and after Beam Failure Detection (BFD) only when beam misalignment between the Tx and Rx occurs, as opposed to every DRX cycle. This technique enables the system to balance the impact of beam measurement and reporting with energy savings during any DRX state.

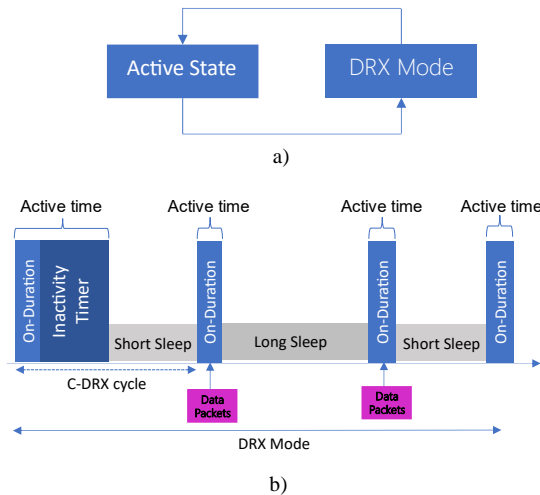


Fig. 1.a) The basic states of LTE, b) DRX states of 5G [6].

Due to the unpredictable nature of data packet arrival and beam misalignment, the DRX-BM scheme's performance analysis is quite complex. To address this issue, we have designed a semi-Markov chain-based mathematical analytic model that describes the Rx behavior and derives the feasible power-saving factor and average delay of the DRX-BM technique. The stationary probability of each operational state and the probabilities of transition between states are computed. Using these probability expressions, we get the power-saving factor, as the length of all sleeping times divided by the total DRX cycle.

The rest of the paper is organized as follows. In Section II, we will cover related work. In Section III, we will introduce miniature 5G communications and the proposal for beam measurement and reporting. In Section IV, we will provide details on DRX-BM. In Section V, we will present the semi-Markov process-based analysis. In Section VI, we will carry out energy-saving factors, and delay estimations to examine the proposed technique. Section VII will cover our conclusions and recommendations for future work.

## II. RELATED WORK

DRX for LTE systems was studied in [7], while many researchers have studied the relationship between DRX sleep duration and energy efficiency [8], [9]. An increase in sleeping time results in the preservation of energy in communications. However, on the other side, it results in an increase in transmission delays. This is because new data packets must wait in Tx buffers for the Rx to switch to an active for data reception. Using adaptive techniques to balance the energy during receiving time and wake-up delay based on a monitoring scheme resulted in the high complexity of the monitoring mechanism. It will require more time and energy on both sides of the link Tx-Rx [10].

In 5G multiple-beam communications, the radio network must manage a vast number of beams. It should derive the UEs to monitor the link for signal strength and exchange several messages before data exchange, which will start after the successful beam pairing. To accomplish this, the PDCCH channel will need to be monitored at shorter intervals and have a reduced sleeping cycle. Consequently, the receiver is given less time to relax and results in a waste of energy. In real communications, the selection of a specific beam pair between the Tx and Rx for data packet transmission often depends on the mobility, positions, and obstacles of mobile devices and serving base stations. The beamforming process will increase data transmission time delays, and external factors related to user mobility will require proper beam alignment.

A beam misalignment event may occur randomly in multiple-beam communication, so the receiver with DRX functionality may lose receiving paging messages at any state. Reducing the sleeping time of sleep states as shown in Fig. 1 b) is proposed in [11], [12]. In this approach, the receiver will perform beam search operations after each cycle, analyzing the whole matrix. Meanwhile, the connection via the LTE network is maintained. Using artificial intelligence (AI), predicting the arrival of

packets from wireless links is proposed in [13]. All these methods can have an impact in terms of energy efficiency in 5G radio networks, but on the other side, it may result in less energy efficiency in the LTE or other wireless networks.

Although the fact that the aligned beam pair may be changed with sufficient frequency, this method may result in additional complications. In real networks where massive MIMO is deployed, there will be a vast number of sharp beams, so making the beam training in every DRX slot for all beams will result in large energy consumption. Even the separation of arrival data processes from the discovery messages will result in good energy efficiency at the sacrifice of delay as proposed in [14] and [15]. Furthermore, the authors explore the possibility that a sleep state of extremely short duration may not be able to maintain optimal energy efficiency. In addition, when the risk of a beam misalignment event is minimal, it may not be necessary to execute the beam training procedure during every DRX cycle in real-network settings. The simulation results confirm the findings, that when the UE velocity is 30 km/h for 256-ms DRX cycle the beam misalignment probability is 20%. By increasing the UE velocity to 60 km/h, it increases to 34% as it reported in [12]. Therefore, if the beam search and reporting functions were added to each DRX cycle, too much energy would be consumed.

DRX in a multi-connectivity setting is addressed in [16] but for the simple scenario of dual connectivity in LTE systems, where the links are not prone to blocking during induced outages. An extended version is proposed by adding an auxiliary active state after each DRX cycle for a low packet arrival rate, in [17]. In this mode, which saves power, user devices can receive packets while they are sleeping up to a certain threshold without going into active mode. Subsequently, user devices can get shorter burst packets right away without a beam search method, which shortens the time it takes to align a beam.

In [18], the DRX scheme of 5G employs the beam training and feedback mechanism, indicating that frequent beamforming is unnecessary in DRX mode. To examine the approach, they employ Poisson modeling considering the self-similarity of the data. The simulation reveals that the energy-saving impact is less than 80%, and the parameters must be adjusted further.

### III. 5G MULTIPLE-BEAM SYSTEM MODEL

We assume a system depicted in Fig. 2 which consists of a 5G BS with three sectorial high directional antennas array each one generates  $M$  beams. Numerous smart UEs with  $N$  beams, which include end-user devices, IoT devices, sensors, and actuators that are network-connected. The network enables periodic messages from BS to UEs that are dependent on data transmission and reception. At a given moment, only one transmitted and received beam pair may be created between BS and receiver. The objective of beamforming is to establish a link between the BS and UEs and locate the optimal beam pair.

In 5G networks, the coverage is beam-based, not cell-based. There is no cell-level reference channel from where the coverage of the cell could be measured. Instead, each cell has one or multiple Synchronization Signal Block (SSB). The user receiver usually deploys a lower number of  $N$  beams to ensure beam alignment with BS from various directions. The SSB beams may be static or semi-static, creating a grid of beams in covering area.

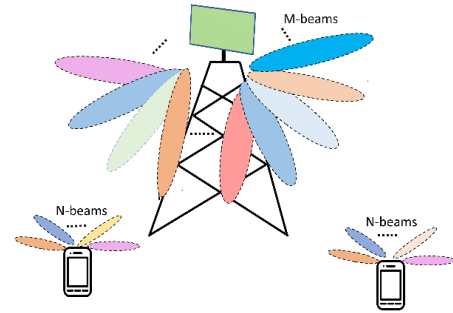


Fig. 2. 5G Multiple-beam communication.

The UEs search and measure the beams, creating a set of candidate beams. The selection of candidate beams is based on the metrics measured, including Reference Signal Received Power (RSRP), Reference Signal Received Quality (RSRQ), and Signal-to-interference-and-noise ratio (SINR) for each beam. After the beam candidate sets up alignment communications, the Rx starts to analyze the subframes based on the time domain. In 5G, the base subframe duration is 1ms [5], which is then divided into slots and symbols based on the numerology [19] and [20]. These subdivisions provide various types of channels to facilitate the exchange of signaling and data transmissions.

Furthermore, the Rx utilizes many synchronization clocks to regulate the durations of various phases. Based on the data traffic model of ETSI [5], data packets destined for a user in a mobile network are generated at random. We will employ the Poisson process for data packets that the receiver decodes with parameter  $\lambda_{is}$  denoted as packet arrival rate. In line with that, the interarrival time between two adjacent packets is denoted by  $t_{ip}$ , which obeys an exponential distribution with a mean value of  $1/\lambda_{is}$ . During the Active state the Tx and Rx can normally exchange the signaling data, and if any packet arrives, the Rx decodes the PDCCH channel and receives data in the minimum time [21]. This indicates that the UEs beam is properly aligned with any of the  $M$  beams provided by the BS, and the link measured and reported by both sides, is of good quality.

The link quality at mmWave frequencies can be highly sensitive to factors such as the movement of the UE, presence of obstacles, or other uncertain events in the environment. As a result, these links are prone to deterioration, potentially reaching an unacceptable level of quality. In these cases, one of the link signals will deteriorate, and beam misalignment is inevitable. In the Active state mode, the user receiver actively monitors the RSRP and RSRQ from the transmitter. If a deterioration in the link quality is detected based on these measurements, it triggers the state-to-beam failure recovery procedure, as described in references [22] and [23]. This recovery procedure aims to address the beam failure and restore the communication link to an acceptable state. In such a circumstance, the receiver is expected to monitor the serving cell and evaluate the downlink quality. During this interval, the data will remain in Tx buffers. Following the study in [18], we assume that beam misalignment occurrences follow a Poisson process with parameter  $\alpha$ , denoting the beam misalignment rate. The time between two successive misalignment occurrences (denoted by  $t\alpha$ ) follows an exponential distribution with a mean value of  $1/\alpha$ . This

misalignment interval  $\tau_\alpha$  is independent of the data packet arrival interval  $t_{ip}$ .

As no beam is properly aligned to allow the data transfer, the UE will continuously search for SSBs or Channel State Information-Reference Signals (CSI-RSs), starting the process of beam training. The Rx connection state, idle or active, determines the starting process of the beam training procedure. For  $M$  transmitted beams and  $N$  receive beams, each of the  $M$  beams is transmitted  $N$  times from gNB (gNB: next Generation NodeB). This ensures that each transmit beam is received over the  $N$  receive beams. The receiver will determine the best beam by utilizing the SSBs and CSI-RS transmitted by the Tx, as described in references [24] and [25]. In 5G NR, the SSBs and CSI-RS are predefined signals that make use of dedicated communication resources. These signals are used for estimating the quality of the transmitter-receiver (Tx-Rx) beam pairs.

In recent years, several beam training techniques with varying energy and time requirements have been proposed and developed. A beam tracking scheme based on deep learning is proposed to flexibly adjust the angular range of beam tracking and spatial correlation among different beams based on the user-specific speeds in [26] and [27]. This scheme aims to reduce the tracking overhead, minimize the tracking time, and ultimately lead to energy reduction and average delay reduction. In [28], it is proposed to use a convolutional neural network (CNN)-based beam selection method that is trained on a simulator-generated beam dataset. This method skips connections and optimizes hyperparameters to find a balance between accuracy and computational complexity. The method is further refined by introducing a fusion learning approach that utilizes two parameters, CSI, and user locations in [29]. This refinement aims to reduce the beam overhead by optimizing the beam prediction output. All the proposed techniques use advanced machine learning, and the complexity of the techniques requires more time and resources on the UEs and BS sides.

In this study,  $t_m$  represents the time required for the beam training operation. During beam management, if a beam misalignment is detected and an aligned beam pair is determined, the receiver side will take  $t_r$  milliseconds to report this information to the BS, as stated in reference [30]. Even in this case, we have a small possibility that communication will not be established between the BS and the user as the movement and other parameters can still deteriorate the link. Alternatively, the reported message may have been compromised meantime.

Following that we describe in Part I that the DRX cycle is split: a) in Active state, where the Rx in continuous mode read the PDCCH channel, and in case of data packets reads the slots of his data directed; b) in Sleep states, where a good part of radio frequency circuits is disabled.

In [10], [18], authors propose the insertion of two extra states into the Active state of the DRX cycle to address the possibility of beam misalignment in multiple-beam systems. But so far, the inclusion of these two stages in the Active DRX cycle shortens the Sleep state. And therefore, the energy consumption might be significantly more than that of the LTE DRX scheme, particularly when the number of Tx and Rx beams is considerable, like in massive 5G NR network.

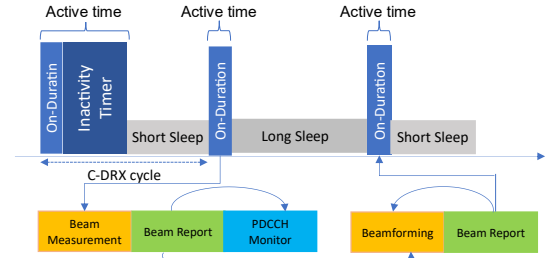


Fig. 3. DRX-BM technique.

In 5G Release 16 and 17, the introduction of Paging Early Indication (PEI) has been implemented [31]. PEI serves the purpose of providing advanced notification to the UE and reducing the number of failed paging occasions (PO). Paging occasions indicate to the UE when it should decode the paging control messages. These enhanced methods focus on conserving energy during idle and inactive modes by increasing the sleep cycle. Another improvement is the insertion of Wake-Up Signal (WUS), the gNB sends WUS before the scheduled arrival time of the data. This gives the UE enough time to wake up, establish a connection with the gNB, and prepare to receive the data.

We propose an energy factory value (EFV) by inserting it into SSBs. EFV will serve as the threshold value for the beam measurement (DRX-BM) technique based on DRX. It takes less processing time for the Rx to measure the beam instead of the PO monitor at the end of the short sleep. The value of the threshold power  $Th_0$  compared with any of the beam's reference signals will decide whether the beam is aligned or not. If it is less than  $Th_0$ , it is misaligned, and beamforming must be performed.

In our approach, we consider all states of DRX, and during the Active time state, the beam measurement is outlined. Additionally, after short and long sleep periods, two short durations are allocated to anticipate the measurement and beamforming actions in case of beam misalignment occurrences. As shown in Fig.3, if a beam misalignment happens after a short sleep of the Rx, it should activate the beam search procedure.

The proposed mechanism DRX-BM will lead the Rx not to measure all beams. The measurement will stop when the threshold value  $Th_0$  is hit, and the procedure continues with reporting and the PDCCH decoding. If the Rx measurements did not find the proper beam value  $Th_0$ , Rx will start the full beam management starting by beam sweeping. After PDCCH is decoded, the Rx enters an Active state to see for his data or can go to a long sleep to preserve energy. If misalignment happens after the long sleep the Rx must do the beam training and the report, in this case, the WUS signal is decoded first by Rx, if the signaling tells Rx to decode the DPCCH for packet data arrival otherwise it will restart the long cycle again. In the other cases where there was no misaligned beam detected, the DRX-BM will continue the flow states as a normal DRX.

#### IV. DRX-BM SEMI-MARKOV CHAIN DESCRIPTION

We model the DRX-BM as an eight-state semi-Markov model, as shown in Fig. 4. As the time between state transitions is a random process, semi-Markov is employed for the analysis of DRX.



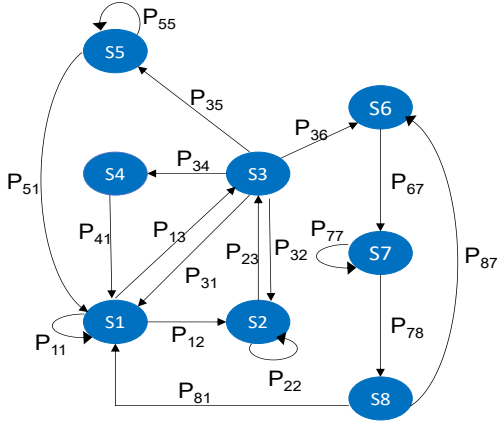


Fig. 4. Semi-Markov chain diagram for the proposed DRX-BM.

Let us start with the first active state, S1. In this state, S1, the UE receives data and monitors the downlink control channel. It remains in the same condition during the end-of-inactivity timeout ( $t_i$ ). In 5G technology, DRX is differentiated by various standard DRX variables. This includes the inactivity timer. It specifies the number of consecutive PDCCH subframes after successfully decoding a PDCCH indicating a new up-link (UL) or downlink (DL) user data transmission for this UE. The UE starts/restarts this timer every time PDCCH indicates a new UL or DL transmission, and UE stays in an active state and keeps monitoring for PDCCH until the expiry of this timer. Once the inactivity timeout has expired without any data, Rx may enter to short-sleep or long-sleep mode. Rx transitions to a brief S3-ready mode if no packets arrive and the inactivity timeout expires. Beam misalignment is an inevitable process of 5G NR millimeter wave communication. As the beam misalignment event may occur also during the active state S1, the receiver must transit to the S2 state, Beam Measurement followed by Report stages will make the beam aligned. If no data is directed for Rx after the beam is realigned, go to the ready state S3, and begin the inactivity time.

State S3 is the ready state until the inactive time expires. We inserted this state to split the active state during the data received and the inactive durations when the Rx is monitoring the PDCCH for data packets. Following the above discussions, four scenarios might cause the Rx's operational status to change. The first one is that the data packet may arrive during this period, and the receiver restarts the inactivity timer. In the new radio 5G, the DRX allows the RX to relax, deferring the sleep states to a micro, short, and long sleep. We will only consider the short and long sleep states, as microsleep has a maximum of 6ms set, and is less effective in terms of energy. If the inactive time has expired, the possible states are S4 long-sleep or S6 short-sleep. In the fourth case, a beam misalignment event occurs before new data arrives. The Rx must start the beam measurements followed by a report to align the beam.

S4 (long-sleep state): Rx enters S4 when the inactivity cycle timer expires ( $t_i$ ). This stage provides a longer period of sleeping time  $t_i$  than the short-sleep state S6. After the termination of the long sleep cycle time, the Rx transits to the S1 state, which will preserve the increase in the average delay.

S6 (short-sleep state): In this state, the Rx sleeps throughout the paging cycle. After the expiration of the paging cycle, the Rx

transitions to S7 to monitor the control channel. If a beam misalignment occurs, ending the time cycle  $t_s$ , Rx should transit to S7 to make the measurement and report align to the beam.

S2, S5, and S7 (beam training and report): In these states, the Rx loses the aligned beam (the signal level results in a less than the threshold value  $Th_0$ ). The Rx scans the SSBs and evaluates the reference signal of available beams to align the optimal beam pair. Depending on the previous transited states, the successor state will be the ready state S3 or S8, in the case of S5, the next state will be the active state S1.

In the ready S8 state, where the UE listens for any incoming data, the duration of the time cycle in this state is  $t_p$ . If any data arrives during this time, Rx transits to the active S1 state and continues to receive the packets. Otherwise, at the expired page cycle  $t_p$ , the Rx should transit to short-sleep S6 to preserve the energy.

The next part presents the stationery and transition probabilities/estimations of the proposed model.

## V. ANALYTICAL MODEL

We analytically compute the stationery and transition probabilities of the proposed DRX-BM mechanism for multiple-beam communications. Additionally, we estimate the power-saving factor and average delay for the proposed DRX-BM mechanism. We assume that the packet arrivals follow a Poisson distribution of  $\lambda_{is}$  packets per millisecond. The packet interval time follows an exponential distribution with a mean value of  $1/\lambda_{is}$ . By studying Fig.4, a semi-Markov chain with an embedded state transition is obtained. The considered data packet traffic is the ETSI model, which fits more closely to wireless communications. Based on this model, data traffic usually consists of several sessions, with intersession arrival time  $t_{is}$  between. The number of packet calls per session  $N_{pc}$ , is assumed to be a geometric distribution with a mean value  $\mu_{pc}$ . The other parameters of the ETSI model are given in Table I.

The inter-arrival time between two successive packet calls may be the interpacket call idle time ( $t_{ipc}$ ). It has the probability  $P_s = 1 - \frac{1}{\mu_{pc}}$  or the inter-session idle time ( $t_{is}$ ) with the probability  $P_{pc} = \frac{1}{\mu_{pc}}$  based on [9].

In active state S1 of the model, if no packet arrival Rx starts the inactivity timeout and Rx goes to state S3. During the expiration of the active time, two events are possible expiration of the active time. The first one is the beam misalignment, and the Rx states must transit to state S2 (transition S1→S2) with probability P12. Once the Rx in this state initiates the beam search, it should transition to state S3 after beam alignment, triggering the start of the inactivity timer.

TABLE I  
DISTRIBUTION OF ETSI PARAMETERS

Parameter	Distribution	Mean value
Session inter-arrival time $t_{is}$	Exponential	$1/\lambda_{is}$
Packet inter-arrival time $t_{ip}$	Exponential	$1/\lambda_{ip}$
Packet call inter-arrival time $t_{ipc}$	Exponential	$1/\lambda_{ipc}$
Number of packets per call $N_p$	Geometric	$1/N_p$

In state S1, beam is aligned, but with no data arrival, so Rx must transit to S3 (transition S1→S3) with probability  $P_{31}$ . The transition probabilities can be computed as follows:

$$P_{11} = [P_S(1 - e^{-\lambda_{ipc}t_I}) + P_{pc}(1 - e^{-\lambda_{is}t_I})]e^{-\alpha t_I}, \quad (1)$$

$$P_{12} = 1 - e^{-\alpha t_I}, \quad (2)$$

$$P_{13} = (P_{pc}e^{-\lambda_{ipc}t_I} + P_S e^{-\lambda_{is}t_I})e^{-\alpha t_I}. \quad (3)$$

In state S3, before the end of the inactive timeout, there are four possible states. When the beam is misaligned, Rx must transit to state S2 (transition S3→S2) with a transition probability of  $P_{32}$ . If the beam is aligned and there is no data arrival, then transit to long sleep state S4 with a  $P_{34}$  transition probability or to S6 short sleep state. The duration of inactive time is  $t_i$ , so the transition probabilities can be computed as follows:

$$P_{31} = [P_{pc}(1 - e^{-\lambda_{ipc}t_i}) + P_S(1 - e^{-\lambda_{is}t_i})]e^{-\alpha t_i}, \quad (4)$$

$$P_{32} = 1 - e^{-\alpha t_i}, \quad (5)$$

$$P_{34} = [P_{pc}(1 - e^{-\lambda_{ipc}t_i}) + P_S(1 - e^{-\lambda_{is}t_i})][1 - e^{-\alpha t_i}], \quad (6)$$

$$P_{35} = 1 - e^{-\alpha t_i}, \quad (7)$$

$$P_{36} = (P_{pc}e^{-\lambda_{ipc}t_i} + P_S e^{-\lambda_{is}t_i})e^{-\alpha t_i}. \quad (8)$$

In state S4 at the end of the timeout cycle, the state is the active state S1, and the probability is 1.

$$P_{41} = 1.$$

In state S6 within the sleep timeout  $t_s$ , if the beam is misaligned, then transit to state S7 with transition probability  $P_{67}$ .

$$P_{67} = 1 - e^{-\alpha t_s}. \quad (9)$$

In the beam search states of S2, S5, and S7, if the beam will align successfully, then transit to the sleep-ready states of S3 in the case of S2, S1 in the case of S5, or S8 in the case of S7 state. These three possibilities help to extend the sleep time and the energy consumed overall. The transition probabilities are as follows:

$$P_{22} = P_{55} = P_{77} = \frac{1}{\mu_\alpha}, \quad (10)$$

$$P_{23} = P_{51} = P_{78} = 1 - \frac{1}{\mu_\alpha}. \quad (11)$$

The UE is inactive in state S8 during the  $t_p$  inactive time, having transited from the beamforming S7 state. If data arrives at UE, it transits to the S1 active state; otherwise, if no data arrives, it goes to the short sleep state S6. The transition probabilities are as follows:

$$P_{81} = [P_{pc}(1 - e^{-\lambda_{ipc}t_p}) + P_S(1 - e^{-\lambda_{is}t_p})]e^{-\alpha t_p}, \quad (12)$$

$$P_{87} = (P_{pc}e^{-\lambda_{ipc}t_p} + P_S e^{-\lambda_{is}t_p})e^{-\alpha t_p}. \quad (13)$$

The state transition probability matrix  $P$  for the proposed DRX-BM technique, as shown in Fig.4, is summarized as follows:

$$P = \begin{bmatrix} P_{11} & P_{12} & P_{13} & 0 & 0 & 0 & 0 & 0 \\ 0 & P_{22} & P_{23} & 0 & 0 & 0 & 0 & 0 \\ P_{31} & P_{32} & 0 & P_{34} & P_{35} & P_{36} & 0 & 0 \\ P_{41} & 0 & 0 & 0 & 0 & 0 & 0 & 0 \\ P_{51} & 0 & 0 & 0 & P_{55} & 0 & 0 & 0 \\ 0 & 0 & 0 & 0 & 0 & 0 & P_{67} & 0 \\ 0 & 0 & 0 & 0 & 0 & 0 & P_{77} & P_{78} \\ P_{81} & 0 & 0 & 0 & 0 & 0 & P_{87} & 0 \end{bmatrix}. \quad (14)$$

With the above state transition probability matrix, the stationery distribution  $\pi_i$  of each state may be calculated using the following formula:

$$\begin{cases} \sum_{i=1}^8 \pi_i = 1 \\ \sum_{j=1}^8 P_{ij} \pi_i = \pi_j \end{cases}. \quad (15)$$

Following the studies of the DRX scheme in LTE [32] and [33] the power saving factor of the user is defined as the ratio of the time spent by the NB-IoT user in the sleep states to the total time spent across all the states. After computing the transition state probabilities and the steady times, as given by Equation (16).

$$PS = \frac{\pi_3 H_3 + \pi_4 H_4 + \pi_6 H_6 + \pi_8 H_8}{\sum_{i=1}^8 \pi_i H_i}. \quad (16)$$

The power saving factor specifies the possibility that the Rx is in Sleep mode at any given moment. A higher value of  $PS$  indicates that the Rx shuts down its receiving circuit more frequently. As a result,  $PS$  presents the energy efficiency that may be achieved.

During the states S2, S5, and S7 the Rx must make the beam search and report and the other procedure to align the beam. All these processes will inevitably take a certain amount of time. The beam time training factor can be derived as

$$\beta = \frac{\pi_2 H_2 + \pi_5 H_5 + \pi_7 H_7}{\sum_{i=1}^8 \pi_i H_i}, \quad (17)$$

$\beta$  is termed as the beam training consumption factor and will be utilized to compute the power efficiency and transmission latency in performance analysis.

The DRX-BM sleep technique will apparently result in a certain transmission delay since certain data must be saved in the Tx cache before being sent to the Rx. Let's denote  $D$  as the average delay across one transmission cycle of the proposed technique since inter-packet call idle time and intersession idle time are exponentially distributed random variables. As of these two times, the arrival events are random observers of the sleep duration and beam search [18]. Thus, the combined average delay resulting from sleep states  $d_s$  and beam measurements  $d_M$  contributes to the overall total average delay.

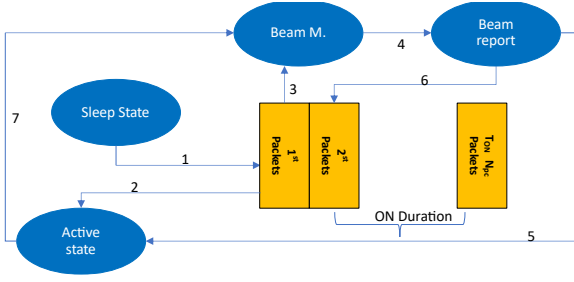


Fig. 5. State transitions related to the delay.

$$D = Ps d_s + \beta d_m. \quad (18)$$

By analyzing Fig.5 and considering that packet arrivals are Poisson distributions, the delay  $d_s$  after sleep states can be derived as:

$$d_s = \frac{t_{dsc} + t_{lsc} + t_i}{2} e^{-\alpha(t_{dsc} + t_{lsc} + t_i)}. \quad (19)$$

Analyzing the beam misalignment, followed by beam training in every state S2, S5, and S7 the average delay can be derived as:

$$d_m = \left( \frac{t_{dsc} + t_m + t_f}{2} + \frac{t_b + t_f}{e^{-\alpha t_f}} \right) [1 - e^{-\alpha(t_{dsc} + t_m + t_f)}], \quad (20)$$

where  $t_b$  is the time of beamforming,  $t_m$  is the time of beam measurement,  $t_{lsc}$  is the length of the short sleep timer and is  $t_{dsc}$  the length of the long sleep timer.

Substituting Equations (19) and (20) into (18), provides our DRX-BM scheme's overall wake-up latency.

There is a compromise between power efficiency and average delay time. Adjusting system settings (such as extending the short or long-sleep time cycle, and beam training) to enhance energy efficiency will unavoidably increase transmission delay. In the next part, through different simulations for a certain value of misalignment rate, and beam search times, our DRX-BM achieves a significantly better tradeoff between power-saving energy and average delay.

## VI. SIMULATION AND ANALYSIS

To validate the proposed technique, simulations are conducted using a MATLAB-based simulator. These simulations aim to compare the numerical findings with the analytical results for different packet arrival rates  $\lambda_{is}$ . By conducting this comparison, the performance and accuracy of the proposed technique can be evaluated across various scenarios. The simulation settings are selected to reflect a realistic set of DRX parameters, as specified in [34].

To examine the performance of DRX during the beamforming, we assumed an inactivity timer  $t_i = 50$  milliseconds (ms), misalignment rate  $\alpha = 1/1000$ , an active period of  $t_0 = 1$  ms, short sleep timer  $t_{lsc} = 560$  ms, long sleep timer  $t_{dsc} = 2560$  ms, and a number of short sleep cycles of 4 and a paging cycle which is 128 ms. To evaluate the number of beams at the gNB and the UE, we consulted the research presented in [35].

TABLE II  
PERFORMANCE PARAMETERS

No.	Parameter	Value
1	Beamwidth	7.5°
2	Number of beams per sector	16
3	Packet arrival rate ( $\lambda_{is}$ )	1/20;1/10;1/3;5
4	Inter-packet call rate ( $\lambda_{ipc}$ )	10
5	Subframe length	1ms
6	Inactivity timer ( $t_i$ )	10-2560ms
7	Short cycle duration ( $t_{lsc}$ )	10-640ms
8	Long cycle duration ( $t_{dsc}$ )	255-2560
9	Active time	1-1600ms
10	Paging cycle	128

We analyzed three sectors at gNB, each containing sixteen beams with a beamwidth of 7.5, and eight beams at the receiver side user mobile are randomly distributed per each sector. The UE must sweep one of the 128 beams (16x8) to obtain the optimal beam pair. The remaining parameters and tuned values are listed in Table II.

This study aims to demonstrate the impact of misalignment on power savings in the UE. Under the present DRX for 5G, the UE must execute beam scanning even if no data packet or paging is available. We propose to insert beam searching and report, as shown in Fig.3, and permit the Rx to perform beam training if beam misalignment occurs. This allows a fresh communication link to be formed once a beam misalignment incident has occurred. However, as mentioned in Section I, beam misalignment can happen often in practice. It depends how fast the UE is moving, the environment changes, and what obstacles are in its way.

It may not be essential for the Rx to execute beam training on every cycle, which wastes system resources. Depending on the relaxation factor K, which can be chosen among the values 1-8, [34], the UE will measure the signal threshold  $Th_0$ . If the paging messages show a lack of data, the Rx can transit to sleep without undertaking an intensive beam search. Although it looks like merely beam searching, large power savings are anticipated. This is because the UE must transition to this state often, after each short/long sleep-in linked mode DRX and after its released mode. To understand the advantages of our proposal, we examine two situations:

- The UE makes the complete beam searching to find the best beam of a cell. This process will take a maximum of time of  $t_b$ .
- By using our proposed approach, a complete beam search is not required. As the Rx detects the threshold value  $Th_0$  in periodical SSBs transmitted, a minimum of time  $t_b$ .

In Fig.6 and Fig.7 respectively, we show the power saving factor against the inactivity time using the maximum beam search time  $t_b(\max)$  and the lowest beam search time  $t_b(\min)$ , with a changing inactivity timer  $t_i$  (10-2560 milliseconds), for various packets arrival rates. Fig. 6 shows the presence of the threshold measurement value of beam searching  $Th_0$ , while Fig.7 shows its absence. Thus, the beam search time for Fig.6 is the maximum beam search time  $t_b \max$ . Instead, the beam search time for Fig.7 is the minimum beam search time  $t_b \min$ . The UE has more opportunities to sleep when  $Th_0$  is not present, which allows for greater power savings. In the event of a maximum

beam search, however, the sleep time decreases, resulting in fewer power savings. The short sleep timer is set to  $t_{\text{isc}} = 560\text{ms}$ , the long sleep cycle to  $t_{\text{dsc}} = 2560\text{ms}$ , the number of short sleep cycles to 4, and the active duration to  $t_0 = 1\text{ms}$ . We can observe from Fig. 6 and Fig. 7, that as the inactivity timer increases, the power saving factor and delay decrease. As the inactivity timer increases, the UE remains in an active state for a longer period, resulting in less power-saving. By increasing the packet arrival rate, the power saving factor for both instances becomes comparable. A high arrival rate indicates that  $Th_0$  is present, requiring complete beam scanning for the UE to transition to the active mode. With inactivity timers greater than 500ms, the power savings and delay for  $\lambda_{\text{is}} = 5$  approaches zero. Due to the high arrival rate and long value of the inactivity timer, the UE cannot transition to the sleep state. By comparing Fig. 6 and Fig. 7 it is observed that for arrival rate of  $\lambda_{\text{is}} = 1/20$ , the power saving achieved by the case of  $t_b$  min is on average 7% higher than the case of  $t_b$  max. The power saving achieved with  $t_b$  min for a packet arrival rate of  $\lambda_{\text{is}} = 5$ , is on average 14 % higher than in the case of  $t_b$  max.

Fig. 8 and Fig. 9, respectively, present the power savings factor against the durations of the sleep timer in two cases when the process of beamforming occurs in the maximum beam search time  $t_b$  max with different packet arrival rates. The short sleep cycle ranges between 128 to 640ms, while the long sleep cycle range is set from 500 to 2560ms. When the duration of the short sleep cycle increases, it also boosts the UE's sleep time, increasing the power savings factor.

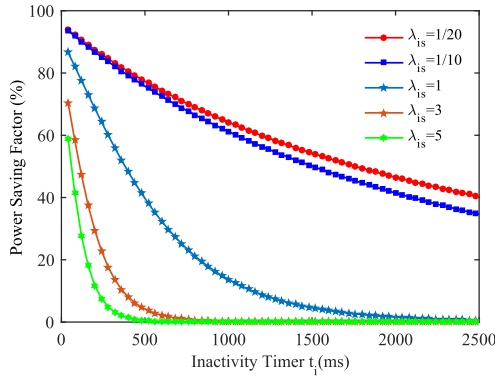


Fig. 6. Power Saving Factor versus inactivity time with different  $\lambda_{\text{is}}$ .

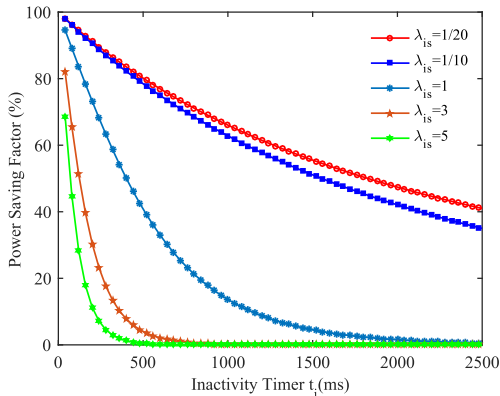


Fig. 7. Power Saving Factor versus inactivity time with different  $\lambda_{\text{is}}$ .

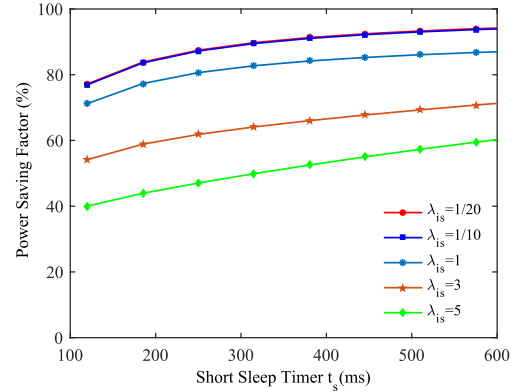


Fig. 8. Power Saving Factor versus Short Sleep Timers.

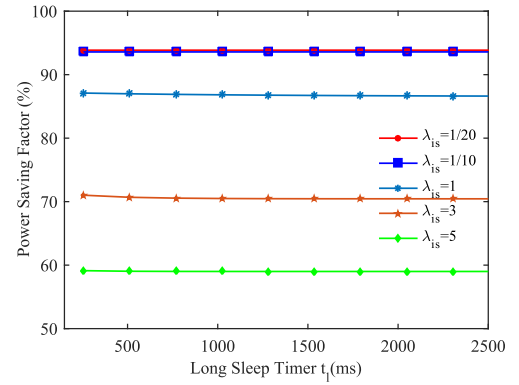


Fig. 9. Power Saving Factor versus Long Sleep Timers.

Fig. 8 and Fig. 9 reveal that the power saving factor decreases as the arrival rate rises. For arrival rate  $\lambda_{\text{is}} = 1/20$ , the power saving factor in Fig. 8 varies between 74% and 95%. As a low arrival rate increases UE sleep duration,  $\lambda_{\text{is}} = 1$  achieves a 37% higher reduction in power consumption than  $\lambda_{\text{is}} = 5$ . As the beam searching time is decreased, for  $t_b$  min achieves 16% greater power savings compared to  $t_b$  max, as shown in Fig. 9.

In scenarios where there is no data or paging, the DRX-BM-based strategy achieves 16% higher energy savings compared to the approach without these techniques. When using DRX without  $Th_0$ , the beam search time remains constant at  $t_b$  max. However, with our proposed DRX-BM technique, the time spent on beam search can be reduced to  $t_b$  min when there are no data packets or paging for the Rx. By reducing the beam search time, the Rx is provided with increased opportunities to enter sleep mode, resulting in enhanced energy savings.

The analysis of Fig. 10 reveals that the DRX-BM technique achieves energy savings at the expense of increased delay. Longer paging cycles result in higher average delay as the UE's reported latency varies due to the extended duration of the paging event. Similarly, Fig. 11 demonstrates the delay experienced by the UE when adjusting the inactivity timeout. Increasing the inactivity timeout leads to a reduction in delay since the UE remains active for a longer duration. Notably, for a packet arrival rate ( $\lambda_{\text{is}}$ ) of 5, a delay of zero is observed after an inactivity time of 480ms, primarily because a higher arrival rate prevents the Rx from entering a sleep state.



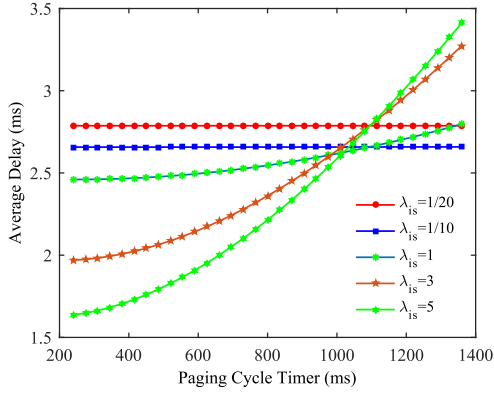


Fig. 10. Average Delay under different Paging Cycle Timers.

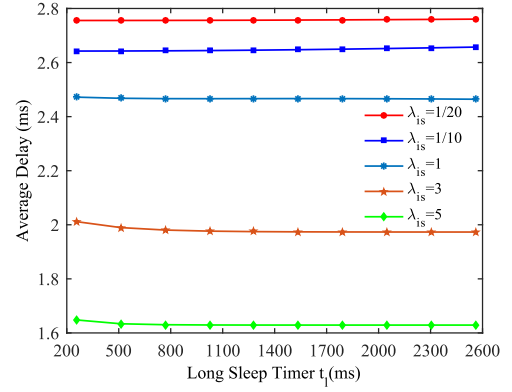


Fig. 13. Average Delay under different Long Sleep Timer.

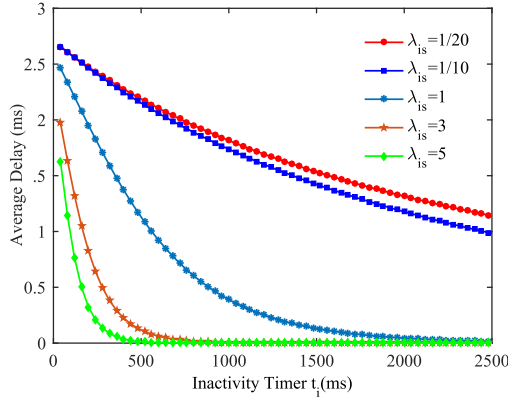


Fig. 11. Average Delay under different Inactivity Timers.

Delay against varying short and long sleep cycles is presented in Fig.12 and Fig.13 respectively. The delay noticed by UE increases as the length of the sleep cycle rises since a longer sleep cycle delays the transition to an active state. The delay measured in the UE decreases as the arrival rate increases. The reason is that the Rx has a smaller chance to enter any of the sleep states. It must respond quickly when new data packets arrive at the Rx. Certainly, this also reduces the power-saving factor, as previously reported.

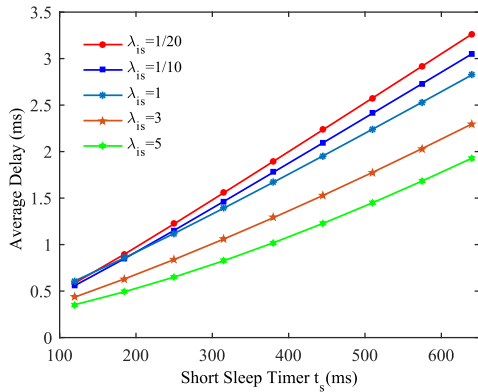


Fig. 12. Average Delay under different Short Sleep Timers.

The similarity between the observed patterns and those of actual 5G networks lends credence to our study findings. In addition, it is evident that including the DRX-BM in the Rx receptions process for 5G networks would result in large power savings. It is evident from Fig. 10 to 13 that the DRX-BM technique obtains significantly lower transmission latency than other full-beam searching methods in wireless multiple-beam communications.

## VII. CONCLUSION AND FUTURE WORK

In this paper, we have proposed a novel DRX-BM technique for energy savings in multiple-beam 5G communications. Next, we propose a semi-Markov-based energy efficiency model for UE in 5G to conserve the device power in case of beam misalignment during the connected mode. In comparison to typical DRX methods, it permits the Rx to often cut off its receiving circuit to achieve discontinuous reception and to undertake beam training only when beam misalignment occurs.

Comprehensive simulation results have demonstrated that our technique achieves a much better balance between energy efficiency and data transfer delay compared to existing methods. Numerical results show that the power saving factor increases up to 95% with a minimum added delay of 15%.

This work will serve as a base for future works which will lead us to choose in an intelligent way from different DRX parameters based on data traffic service type. The work can be further extended by optimizing performance parameters and improving energy efficiency while maintaining the delay experienced by the 5G users.

## REFERENCES

- [1] "Ericsson Mobility Report," Ericsson, June 2022.
- [2] "ITU-R M.2083: Framework and Overall Objectives of the Future Development of IMT for 2020 and Beyond," Sep. 2015.
- [3] M. Agiwal, A. Roy and N. Saxena: "Next Generation 5G Wireless Networks: A Comprehensive Survey," in *IEEE Communications Surveys & Tutorials*, vol. 18, no. 3, pp. 1617-1655, third quarter 2016.
- [4] E. Dahlman, S. Parkvall, and J. Skold, "4G LTE-Advanced Pro and The Road to 5G", Elsevier, ch. 10, pp. 269-283, 2016.
- [5] "TS 36.3003, ETSI, LTE: Evolved Universal Terrestrial Radio Access (E-UTRA) and Evolved Universal Terrestrial Radio Access Network(E-UTRAN), Overall description," V. 11.9.0, 2014.
- [6] "TS38.304, 3GPP: User Equipment (UE) Procedures in Idle Mode and RRC", V. 16.7.0, 2021.

- [7] Y. Y. Mihov, et al. "Analysis and performance evaluation of the DRX mechanism for power saving in LTE," in IEEE 26-th Convention of Electrical and Electronics Engineers, pp. 520-524, 2010.
- [8] H. -L. Chang, S. -L. Lu, T. -H. Chuang, C. -Y. Lin, M. -H. Tsai and S. -I. Sou, "Optimistic DRX for machine-type communications," IEEE International Conference on Communications (ICC), pp. 1-6, 2016.
- [9] S. Fowler, A. O. Shahidullah, M. Osman, J. M. Karlsson and D. Yuan, "Analytical evaluation of extended DRX with additional active cycles for light traffic", Computer Networks, Vol. 77, pp 90-102, 2015.
- [10] F. Yi, Y. Ji, Z. Lao and J. Wang, "An Enhanced Discontinuous Reception Mechanism for Power Saving in 5G", IEEE 92nd Vehicular Technology Conference (VTC2020-Fall), pp. 1-5, 2020.
- [11] S. W. Kwon, J. Hwang, A. Agiwal and H. Kang, "Performance analysis of DRX mechanism considering analogue beamforming in millimeter-wave mobile broadband system," 2014 IEEE Globecom Workshops, pp. 802-807, 2014.
- [12] M. K. Maheshwari, M. Agiwal, N. Saxena and A. Roy, "Directional Discontinuous Reception (DDRX) for mmWave Enabled 5G Communications," in IEEE Transactions on Mobile Computing, Vol. 18, No. 10, pp. 2330-2343, 2019.
- [13] M. M. Latif, M. K. Maheshwari, N. Saxena, A. Roy, and D. Ryeol Shin, "Artificial Intelligence-Based Discontinuous Reception for Energy Saving in 5G Networks" Electronics 8, No. 7: 778, 2019.
- [14] F. Moradi, E. Fitzgerald and B. Landfeldt, "Modeling DRX for D2D Communication," in IEEE Internet of Things Journal, Vol. 8, No. 4, pp. 2574-2584, 2021.
- [15] S. H. A. Shah, S. Aditya and S. Rangan, "Power-Efficient Beam Tracking During Connected Mode DRX in mmWave and Sub-THz Systems," in IEEE Journal on Selected Areas in Communications, Vol. 39, no. 6, pp. 1711-1724, June 2021.
- [16] M. K. Maheshwari, M. Agiwal, N. Saxena and A. Roy, "Hybrid Directional Discontinuous Reception (HD-DRX) for 5G Communication," in IEEE Communications Letters, Vol. 21, No. 6, pp. 1421-1424, 2017.
- [17] N. R. Philip and B. Malarkodi, "Extended Hybrid Directional DRX with Auxiliary Active Cycles for Light Traffic in 5G Networks", Transactions on Emerging Telecommunications Technologies, 2018.
- [18] D. Liu, C. Wang and L. K. Rasmussen, "Discontinuous Reception for Multiple-Beam Communication," in IEEE Access, Vol. 7, pp. 46931-46946, 2019.
- [19] "TR 38.802 V2.0.0, 3GPP: Study on New Radio (NR) Access Technology Physical Layer Aspects," V.14.2.0, 2017.
- [20] "TR 38.804 V1.0.0, 3GPP: Study on New Radio Access Technology Radio Interface Protocol Aspects," V. 14.2.0, 2017.
- [21] "TS 38.101-1, 3GPP: NR User Equipment (UE) Radio Transmission and Reception Part 1," V15.4.0, Dec. 2018.
- [22] "TSG RAN WG1, 3GPP: Meeting 90 R1-1712702 Std Radio Link Monitoring," 2017.
- [23] "TSG RAN WG1, 3GPP: Meeting 90 R1-1712224 Procedure RDetails for Beam Failure Recovery," 2017.
- [24] "TSG-RAN WG1, 3GPP: Reference Signals and Reports to Support Beam Management," 2016.
- [25] "TSG RAN WG1, 3GPP: Beam Selection CSI Acquisition for NR MIMO," 2016.
- [26] K. Ma, H. Zou, C. Sun and Z. Wang, "Deep Learning Assisted Adaptive mmWave Beam Tracking: A Sum-Probability Oriented Methodology," IEEE Global Communications Conference, pp. 573-578, 2022.
- [27] Z. Wang et al., "Intelligent Beam Training with Deep Convolutional Neural Network in mmWave Communications," IEEE Global Communications Conference, pp. 1223-1228, 2022.
- [28] S. K. Vankayala, S. Kumar, T. D. A. Mathur, S. Yoon and I. Kommineni, "Deep-Learning Based Beam Selection Technique for 6G Millimeter Wave Communication," IEEE 33rd Annual International Symposium on Personal, Indoor and Mobile Radio Communications (PIMRC), pp. 1380-1385, 2022.
- [29] S. Yang, J. Ma, S. Zhang and H. Li, "Beam Prediction for mmWave Massive MIMO using Adjustable Feature Fusion Learning," IEEE 95th Vehicular Technology Conference: (VTC2022-Spring), pp. 1-5, 2022.
- [30] A. Huang, K. -H. Lin and H. -Y. Wei, "Beam-Aware Cross-Layer DRX Design for 5G Millimeter Wave Communication System," in IEEE Access, Vol. 8, pp. 77604-77617, 2020.
- [31] "TR 38.840, 3GPP: Study on User Equipment (UE) power saving in NR", V16.0.0, 2019.
- [32] K. Zhou, N. Nikaein and T. Spyropoulos, "LTE/LTE-A Discontinuous Reception Modeling for Machine Type Communications," in IEEE Wireless Communications Letters, Vol. 2, No. 1, pp. 102-105, 2013.
- [33] K. Lien, K. -H. Lin and H. -Y. Wei, "Energy-Efficient Traffic Steering in Millimeter-Wave Dual Connectivity Discontinuous Reception Framework," in IEEE Access, Vol. 10, pp. 115716-115731, 2022.
- [34] "TS 38.133, 3GPP: Requirements for support of radio resource management", V17.1.0, 2022.
- [35] K. -H. Lin, C. -W. Weng and H. -Y. Wei, "Intelligent Directional Paging Framework in Millimeter-Wave 5G NR Systems," in IEEE Transactions on Wireless Communications, Vol. 21, No. 12, pp. 10739-10754, Dec. 2022.



**Olimjon Shurdi** received the Diploma of Electronics Engineering in 1998. In 2009 he completed his Ph.D. in Information and Communication Technologies at the Polytechnic University of Tirana and in 2013 he received the Associate Professor title. Since 1998, he has been a full-time lecturer at the Polytechnic University of Tirana, Faculty of Information Technology. He is the author of numerous articles for several international conferences and journals. His research interests include wireless networks, mobile ad hoc networks, wireless sensor networks, and multimedia communication in next-generation networks.



**Alban Rakipi** received the B.S. degree in 2009 and the M.S. degree in 2011 in Telecommunication Engineering from the Faculty of Information Technology, Polytechnic University of Tirana. He received a second level specializing master's degree in "Navigation and Related Applications" from Polytechnic University of Turin, Italy. He received the Ph.D. degree in Information and Communication Technologies from Polytechnic University of Tirana in 2015. From 2012 he is a full-time lecturer at PUT. His research interests include signal processing, satellite positioning systems and technologies, GNSS applications, integrity monitoring, mobile ad hoc routing algorithms and network protocols.



**Argenti Lala** received BE and PhD degrees from the Polytechnic University of Tirana (PUT) in 1999 and advanced Master in Telecommunication Engineering in 2008. He obtained his Ph.D. from PUT in 2013. From 2008 he has been a Lecturer at the Department of Electronics and Telecommunications, Faculty of Information Technology. His research interests lie in the area of electromagnetic field, wave propagation, transmission, and antennas. In the latest years he has been focused on methods of calculation of the electromagnetic field in the vicinity of the cellular base stations. He has published several papers in referred Journals and International conference proceedings. He is currently lecturer of several subjects including Measurements of the radio frequencies, Antennas, and wave propagation. He is a scientific tutor of master students, while continuing his scientific research.